Storm-Relative Observations in Tropical Cyclone Data Assimilation with an Ensemble Kalman Filter

ALTUĞ AKSOY

Cooperative Institute for Marine and Atmospheric Studies, University of Miami, Miami, Florida

(Manuscript received 29 March 2012, in final form 11 September 2012)

ABSTRACT

A storm-relative data assimilation method for tropical cyclones is introduced for the ensemble Kalman filter, using the Hurricane Weather Research and Forecasting (HWRF) Ensemble Data Assimilation System (HEDAS) developed at the Hurricane Research Division of the Atlantic Oceanographic and Meteorological Laboratory at the National Oceanic and Atmospheric Administration. The method entails translating tropical cyclone observations to storm-relative coordinates and requires the assumption of simultaneity of all observations. The observations are then randomly redistributed to assimilation cycles to achieve a more homogeneous spatial distribution. A proof-of-concept study is carried out in an observing system simulation experiment in which airborne Doppler radar radial wind observations are simulated from a higher-resolution (4.5/1.5 km) version of the same model. The results here are compared to the earth-relative version of HEDAS. When storm-relative observations are assimilated using the original HEDAS configuration, improvements are observed in the kinematic representation of the tropical cyclone vortex in analyses. The use of the storm-relative observations with a more homogeneous spatial distribution also reveals that a reduction of the covariance localization horizontal length scale by ½ to ~120 km provides the greatest incremental improvements. Potential positive impact is also seen in the slower cycle-to-cycle error growth. Spatially smoother analyses are obtained in the horizontal, and the evolution of the azimuthally averaged wind structure during short-range forecasts demonstrates better consistency with the nature run.

1. Introduction

The new frontier in tropical cyclone (TC) data assimilation is at the vortex scale. Improvements in our predictive capacity of the large (synoptic to global) scales of the atmosphere have led to a steady increase in TC track forecast skill, while that in predicting TC intensity has remained virtually unchanged (e.g., Hamill et al. 2011; Berg and Avila 2011). Kaplan et al. (2010) found that the information at the large scales only contributes to 35%–65% of the skill in predicting rapid intensification (RI) for a 25-kt (~13 m s^{-1}) threshold (see their Fig. 17c). This finding motivates the thinking that TC inner-core processes could be responsible for some of the remaining skill in predicting RI. This is also supported by recent research that points to the importance of the asymmetric vortex structure in determining storm evolution (e.g., Reasor et al. 2004; Mallen et al. 2005; Nguyen et al. 2008; Rogers 2010).

The National Oceanic and Atmospheric Administration (NOAA) has been collecting high-resolution airborne observations in TCs for 35 yr using NOAA's WP-3D (P-3) aircraft (Aberson et al. 2006), and for 15 yr around them from its high-altitude Gulfstream IV jet (Aberson 2010). However, only a few studies have explored the value of these TC inner-core data for high-resolution data assimilation. In a proof-of-concept study, Zhang et al. (2009) demonstrated that initial conditions produced by an ensemble Kalman filter (EnKF) using observations from a land-based radar led to more skill than three-dimensional variational data assimilation (3DVAR) in predicting the rapid formation and intensification of a TC. The same data assimilation system was recently tested with airborne Doppler radar observations (Weng and Zhang 2012; Zhang et al. 2011) and demonstrated improvement in the representation of the vortex structure in Hurricane Katrina (2005) as well as a reduction in intensity forecast error in 61 cases from 2008 to 2010 when compared to operational dynamical models.

Corresponding author address: Dr. Altuğ Aksoy, CIMAS, Rosenstiel School of Marine and Atmospheric Science, 4600 Rickenbacker Cswy., Miami, FL 33149.
E-mail: aaksoy@rsmas.miami.edu

DOI: 10.1175/MWR-D-12-00094.1

In a parallel effort, the Hurricane Research Division (HRD) at the NOAA/Atlantic Oceanographic and Meteorological Laboratory has built the Hurricane Ensemble Data Assimilation System (HEDAS), an ensemble-based data assimilation system that utilizes high-resolution observations in and around TCs. HEDAS comprises an EnKF and a version of the Hurricane Weather Research and Forecasting (HWRF) model (Gopalakrishnan et al. 2011). Aksoy et al. (2012, hereafter A12) demonstrated the value of assimilating simulated airborne Doppler radar radial wind data with HEDAS and showed that these observations not only had a direct positive impact on the vortex wind structure in a TC but also an indirect positive impact on the vortex thermodynamic fields.

As documented in A12, HEDAS was originally designed to assimilate available airborne observations during a particular flight in short-range cycles to obtain a final vortex analysis. Observations are typically assimilated in earth-relative coordinates in hourly time windows (48 min in A12), since this is believed to be a good compromise between the need for spatial observation coverage per cycle that is representative of the important atmospheric scales and the need for multiple assimilation cycles to obtain quasi-linear error growth for a balance between the EnKF and the forecast model (Daley 1991, section 6.3). Because observations follow the particular flight pattern, assimilation cycles naturally separate observations into penetration and downwind legs, leading to cycles alternating in how well they sample the TC vortex. The impact of this variability in spatial coverage among cycles is documented in A12.

While the current configuration of HEDAS has led to marked improvements in analyzed vortex structure (A12), the manner in which the observations are assimilated is nevertheless considered to be suboptimal due to the restrictions it imposes on spatial coverage and assimilation window length. One way around this issue could be to assume a steady-state vortex and, then, to assimilate observations arbitrarily from the entire flight, thus distributing them more homogeneously to assimilation cycles.[1] Such an assumption is for example common in ensemble-based radar data assimilations of continental convective storms, where the typical assimilation window length roughly matches the time it takes for the Weather Surveillance Radar-1988 Doppler (WSR-88D) to complete one full volume scan (Dowell et al. 2004).

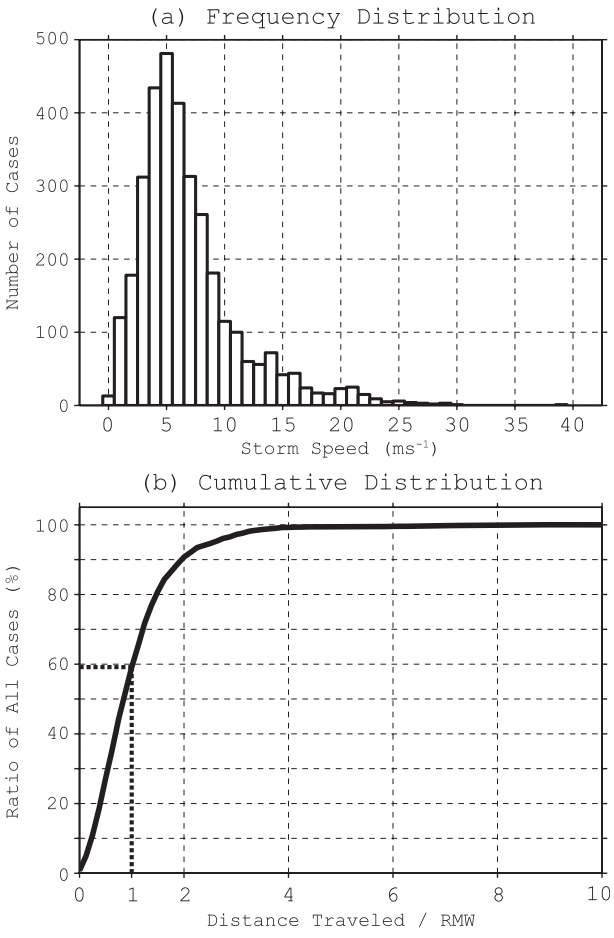

FIG. 1. (a) Frequency distribution and (b) cumulative distribution, as a function of storm speed, for all 1970–2010 Atlantic basin tropical cyclones with central pressure less than 990 hPa. Corresponding distance traveled normalized by RMW is shown as a horizontal scale in the bottom panel. The portion of the distribution that corresponds to storm speeds that result in traveled distances greater than 1 RMW is also highlighted.

However, because a TC can move considerably during a typical 4-h flight,[2] assuming simultaneity of observations from all flight legs may lead to considerable storm-relative position errors in the case of vortex-scale TC data assimilation. This is illustrated in Fig. 1, which

[1] It should be noted that ''simultaneity'' and ''steady state'' here are not used as absolute terms but rather as representative of the relevant important atmospheric scales. Although observations from a flight are unavoidably impacted by the turbulent and convective scales of motion, the primary focus in HEDAS is not to accurately resolve those scales in analyses but rather the ''vortex scale'' at which the azimuthally averaged flow characteristics and low-wavenumber asymmetries are believed to be important. At the vortex scale, variability within a 4-h flight window is assumed to be small, leading to a mostly steady-state storm.

[2] Flights generally are longer than 8 h including ferry time from port to the storm and back. Here, 4 h is representative of the in-storm portion of the flight when observations are gathered.

shows the frequency distribution of all Atlantic tropical cyclones during the period 1988–2010 with central pressure less than 990 hPa as a function of storm speed [from the extended best-track dataset; Demuth et al. (2006)]. The frequency distribution reveals that the mode (most frequently occurring speed) is about 5 m s^{-1} (Fig. 1a).

To represent the maximum possible horizontal displacement for any given observation, a 2-h possible displacement is assumed between observations and the average storm center during a typical 4-h data assimilation period, thus leading to a total distance estimate for the range of storm speeds observed. The total distance estimates are then normalized by the radius of maximum wind [RMW, as estimated in the extended best-track dataset of Demuth et al. (2006) for the same cases in Fig. 1a] for a measure of the significance of storm speed with respect to storm structure.

The RMW, in an azimuthally averaged sense, is a fundamental parameter of storm structure because it indicates the relative positions of the greatest kinematic and thermal gradients within the vortex (Stern and Nolan 2009). It is conjectured that observations with displacements greater than one RMW, should they be assimilated assuming simultaneity, can likely be detrimental to data assimilation, as they would result in large and unrealistic cross-gradient innovations. According to this normalized total distance measure, about 40% of the Atlantic TCs had storm speeds that would lead to observation displacements of at least one RMW (Fig. 1b). In other words, for at least 40% of the Atlantic TC cases, data assimilation would be carried out using observations that are at least one RMW apart. It is believed that there are a significant number of cases where potential issues could exist in obtaining a coherent vortex-scale analysis when observations are assimilated with their earth-relative coordinates. Clearly, the problem also becomes compounded by the fact that in high-resolution data assimilation typical RMWs are resolved by only a few multiples of the horizontal grid spacing. For HEDAS at 3-km grid spacing, a typical RMW of 35 km (roughly the average RMW from the extended best-track dataset for the same Atlantic TCs considered here) corresponds to 12 grid spaces.

The current article explores the potential of assimilating the data within a storm-relative framework. Given vortex-scale stationarity, observations can be assimilated within a storm-relative framework in any assimilation cycle (and not necessarily in the temporal order they are sampled within the vortex), leading to better spatial observation coverage in each cycle. The storm-relative assimilation is also expected to improve HEDAS performance indirectly by allowing for better flexibility in the choice of system characteristics such as covariance localization and covariance inflation. As explained before, in the current HEDAS configuration, the choice of these parameters is dictated more by the nature of the spatial observation distribution than pure optimality concerns.

It should be noted that storm-relative analysis in TCs is not a new concept. Cline (1926) first described in his section 2 elegantly how ''the stations in the storm area are located in their proper geographical positions as related to the path along which the cyclonic center traveled.'' More recently, Weng and Zhang (2012) and Xiao et al. (2009) have carried out data assimilation with observations that are advected geographically following storm motion. However, the application of the concept of simultaneity to observations from a complete flight in TC data assimilation and its ramifications for the relevant scales of motion are novel. As a proof of concept, the observing system simulation experiment (OSSE) framework of A12 is used here. The same reference of ''truth'' as in A12 provides a natural three-dimensional benchmarking environment to evaluate the details of the performance of storm-relative data assimilation. A subsequent paper will focus on results with real data.

The storm-relative framework is described in section 2. Section 3 briefly summarizes HEDAS and the model characteristics as well as explaining the data assimilation experiments performed. Section 4 continues with the presentation of the results; the summary and discussion are in section 5.

2. Storm-relative observation processing

The objective is to assimilate the data within a storm-relative instead of an earth-relative framework. The knowledge of at least two storm center positions is required to determine, by linear translation, the position of the storm center as of the sampling time of a given observation.

For an arbitrary observation from a given flight, the position of the storm center at an observation time is obtained linearly between two neighboring observed storm center locations:

$$c_o = c_1 + (c_2 - c_1)\frac{(t_o - t_1)}{(t_2 - t_1)}, \tag{1}$$

where c stands for the center position (latitude and longitude), subscript o denotes the time of the observation, subscripts 1 and 2 denote neighboring observed storm center locations, and t denotes time. If the sampling time of the observation t_o happens to be outside

the window $[t_1, t_2]$ of the two nearest storm centers, the computation amounts to an extrapolation.

It should be noted that the linear assumption in Eq. (1) has limitations when neighboring storm centers are too far apart in time or when extrapolation is needed to carry out the computation. In the current application of vortex-scale data assimilation at 3-km grid spacing, relevant temporal and spatial scales of storm center oscillations are believed to be those influenced by interactions with shear. As an example, Jones (1995) demonstrates that such shear-induced oscillations occur on a time scale of 6 h. Faster, trochoidal oscillations of the center are also possible, although the spatial scales of such features at 2–4 km (Marks et al. 2008) are too small to be resolved in the current vortex-scale data assimilation configuration. In practice, center fixes during a hurricane flight are routine and reported on ~1-h frequency. Under these circumstances, limitations due to interpolation are not expected to have a substantial negative impact on the overall performance of data assimilation with storm-relative observations.

Once c_o is determined, the position of the observation is translated relative to an overall storm center by maintaining the observation's storm-relative position with respect to c_o. The overall storm center is representative of the TC position at an initial synoptic time of a given model run, as analyzed by the National Hurricane Center (NHC). The position translation is carried out as

$$x_o^* = x_o - c_o + c^*, \tag{2}$$

where x represents geographical location (latitude or longitude) of the datum and the asterisk denotes the overall storm center.

The translation of observations to a storm-relative framework enables the assumption of simultaneity during the flight. To take advantage of this assumption, the observations are randomly assigned to assimilation cycles drawn from a uniform probability distribution within the flight window. This effectively distributes observations evenly to the assimilation cycles.

Figure 2 compares the horizontal, vertical, and temporal distribution of simulated radar superobservations within a storm-relative and an earth-relative framework. In the earth-relative framework, observations are naturally distributed into penetration and downwind legs, as the length of 1-h penetration and 30-min downwind legs roughly coincide with the 48-min assimilation windows. As a result, assimilation windows alternatively contain observations mostly from the vortex inner core and its outer regions. This is differentiated in Fig. 2a between the gray circles (first, ''penetration,'' cycle) and

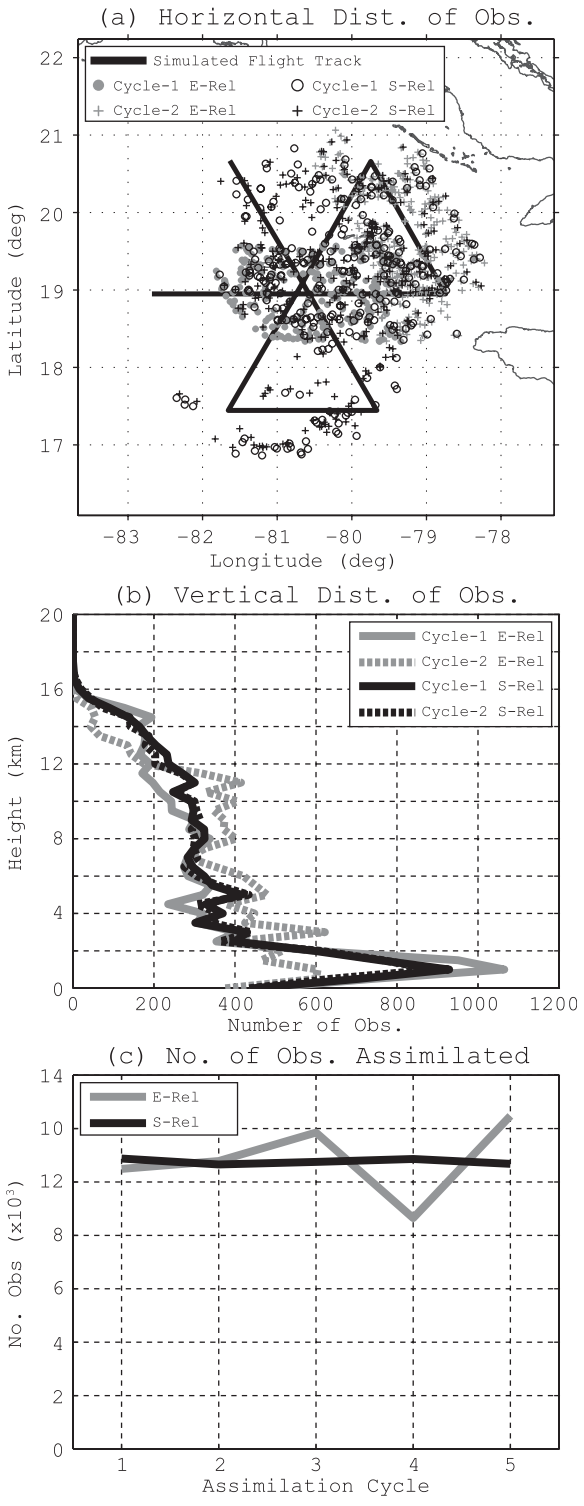

FIG. 2. Comparison of observation distributions in HEDAS with earth-relative and storm-relative observation processing (E-Rel and S-Rel, respectively) (a) in the horizontal near flight level (~3-km altitude), (b) in the vertical, and (c) across assimilation cycles. Odd- (even-) numbered cycles in HEDAS with earth-relative observation processing contain observations from penetration (downwind) legs.

the gray crosses (second, ''downwind,'' cycle). This clearly leads to an asymmetric sampling of the vortex in the various assimilation cycles. Within the storm-relative framework, the observations are distributed to all the cycles, leading to a more homogeneous horizontal sampling of the vortex in the first two assimilation windows (cf. black circles to black crosses).

Observations in a storm-relative framework also exhibit a vertical distribution that is more uniform among assimilation windows than in the earth-relative framework. In Fig. 2b, it is evident that a greater number of boundary layer observations are available in the penetration cycle than in the downwind cycle within the earth-relative framework. This discrepancy is removed in the storm-relative framework. Finally, Fig. 2c shows a greater variability in the total number of observations per cycle in the earth-relative framework, depending on whether or not observations are obtained from a penetration leg and/or whether sufficient cloud liquid water is present to result in radar echoes. Such variability is greatly reduced within the storm-relative framework.

3. Experimental setup

a. HEDAS and experimental HWRF

A thorough discussion of HEDAS and the model configuration can be found in A12. Briefly, HEDAS is an ensemble data assimilation system with a square root EnKF (Whitaker and Hamill 2002). It employs covariance localization with a compactly supported fifth-order correlation function from Gaspari and Cohn (1999). The horizontal localization length scale in the original HEDAS implementation is chosen as 80 grid points (~240 km) to ensure that most of the vortex is updated during each assimilation cycle. To counteract the underestimation of variance, some experiments employ covariance inflation (Hamill and Whitaker 2005) and/or covariance relaxation (Zhang et al. 2004). Observations are assimilated in 48-min windows and only in the inner domain.

The current application uses 30 ensemble members. The initial ensemble perturbations are obtained from operational National Centers for Environmental Prediction Global Ensemble Forecast System analyses. A 6-h ensemble spinup run is carried out to develop appropriate covariance structures relevant to the scales at which the data assimilation is performed.

The experimental HWRF model is configured with 2 two-way-interacting computational domains of 9- and 3-km horizontal grid spacing, respectively. The vortex-following nest motion of the inner domain (Gopalakrishnan et al. 2002, 2006) is suppressed during spinup and data assimilation cycles so that all ensemble members are initialized with collocated inner domains to facilitate gridpoint-based spatial covariance computations in the EnKF.

b. Simulation of airborne radar observations

The same simulated Doppler radar radial wind superobservations (superobs hereafter) dataset is used here as in A12. The nature run that is the basis for these simulated data consists of a model representation of Hurricane Paloma (2008) at double the horizontal resolution (4.5/1.5 km), as in HEDAS. A12 showed that, during the 24-h nature run simulation, the vortex steadily intensified from a tropical storm to a category-2 hurricane. The evolution of the vortex in the nature run was deemed sufficiently realistic in structure and exhibited measurable differences from the model behavior in HEDAS.

The Doppler radar radial wind data are produced by simulating a butterfly-shaped flight pattern within the nature run during the ''mature phase'' of the vortex and then interpolating from model space using a realistic forward operator at 12-min intervals. The superobs data are generated by the same method as that is used in real time (Zhang et al. 2009). Exactly the same observations as in A12 are used here, with the main difference being the implementation of the additional step of converting observations to a storm-relative framework.

c. Description of data assimilation experiments

To test how HEDAS performs within the storm-relative framework, HEDAS analyses using storm-relative observations (the DA_SCTR experiment) are first compared to HEDAS analyses with earth-relative observations as well as the control experiment with no data assimilation (i.e., the DA_BASIC and CTRL experiments of A12, respectively).

A12 demonstrated that the forecast ensemble in HEDAS was deficient in spread. However, due to the limited spatial distribution of the observations in each cycle, the covariance localization length scale had to be chosen to be large enough to update most of the vortex in each cycle. This constraint likely contributed to the limited positive impact in their experiments with covariance inflation and covariance relaxation. As the more homogeneous spatial distribution of observations in DA_SCTR here allows for better flexibility in dealing with ensemble spread deficiency, a more systematic evaluation of the impact of covariance inflation (Hamill and Whitaker 2005) and covariance relaxation (Zhang et al. 2004) techniques is also carried out. Specifically, two experiments with one-half and one-quarter of the

TABLE 1. Summary of the data assimilation experiments.

Expt	Observation processing	Covariance relaxation (% prior)	Covariance length scale (grid points)	No. of observations (% DA_BASIC)
DA_BASIC	Earth relative	None	80	100
DA_STORMCTR	Storm relative	None	80	100
DA_OBNUM50%	Storm relative	None	80	50
DA_OBNUM25%	Storm relative	None	80	25
DA_RELAX25%	Storm relative	25	80	100
DA_RELAX50%	Storm relative	50	80	100
DA_CVLOC1/2	Storm relative	None	40	100
DA_CVLOC1/4	Storm relative	None	20	100

number of observations assimilated as in DA_BASIC (DA_OBNUM50% and DA_OBNUM25%, respectively), two experiments with covariance relaxations of 50% and 75% (DA_RELAX50% and DA_RELAX75%, respectively) as opposed to none in DA_BASIC, and two experiments with covariance localization length scales that are one-half and one-quarter (DA_CVLOC1/2 and DA_CVLOC1/4, respectively) of that in DA_BASIC are carried out. No state-space covariance inflation is applied here. See Table 1 for details.

4. Results

a. Impact of storm-relative data assimilation

The direct impact of the storm-relative data assimilation is investigated first with the same HEDAS configuration as in A12. Consequently, this section is devoted to the comparison of experiments CTRL and DA_BASIC from A12 and the new DA_SCTR with storm-relative data assimilation.

1) OBSERVATION-SPACE DIAGNOSTICS

As in A12, observation-space diagnostics are computed by accumulating various statistics of innovations, or concurrent observation-minus-forecast differences. To be consistent between the experiments, the same earth-relative observation dataset as in A12 is used for evaluation purposes, and these observations are never assimilated in any of the experiments shown here.

Observation-space diagnostics for filter performance are shown in Fig. 3, where various statistics of the prior (forecast) and posterior (analysis) innovations of Doppler radial wind are plotted for each of the assimilation cycles. Innovations in the control run (dotted gray) are believed to be generally random in nature, because mean innovations are much smaller in magnitude than RMS innovations. Mean innovations become even smaller when data assimilation is performed, and the differences are indistinguishable between DA_BASIC and DA_SCTR.

Smooth transitioning from analyses to forecasts is a desired property of a data assimilation system to minimize dynamical shock to the forecast model and the resulting loss of information due to the generation and propagation of inertia–gravity waves (Kalnay 2006, section 5.7). Although the average RMS innovation (Fig. 3b) is not considerably different in DA_SCTR than in DA_BASIC ($\sim$4 m s^{-1}), ''error growth'' appears to be smaller during cycle-to-cycle short-range forecasts in DA_SCTR compared to DA_BASIC: the average increase in RMS innovations within short-range forecasts is 2.5 m s^{-1} in DA_BASIC, as opposed to the much smaller value of 0.6 m s^{-1} in DA_SCTR. This potentially indicates smoother analysis-to-forecast transitions during the short-range forecasts.

In terms of ensemble spread, there appears to be a greater inconsistency between the ensemble spread and RMS innovations in DA_SCTR than in DA_BASIC, which is indicated by the smaller spread sufficiency ratio in DA_SCTR. The spread sufficiency ratio mainly measures how ensemble variability compares to random error (Aksoy et al. 2009). This is believed to be partially the outcome of the more homogeneous horizontal distribution of observations in DA_SCTR than in DA_BASIC. On average, this leads to model grid points in DA_SCTR being updated by observations that are closer to them in distance than in DA_BASIC, thereby reducing the average ''effective'' horizontal localization distance applied per model grid point and increasing the average distance-dependent weight imposed on covariances. These are illustrated in Fig. 4, where the average distance between observations and updated model grid points as well as the resulting average covariance weight imposed during covariance localization per updated model grid point are shown. Especially during the cycles in which observations from downwind legs (denoted with the symbol ''D'' beneath cycle numbers) are assimilated in DA_BASIC, the more homogeneous horizontal distribution of observations in DA_SCTR is believed to lead to the smaller average observation–gridpoint distance and a hence greater average covariance weight applied, compared to the

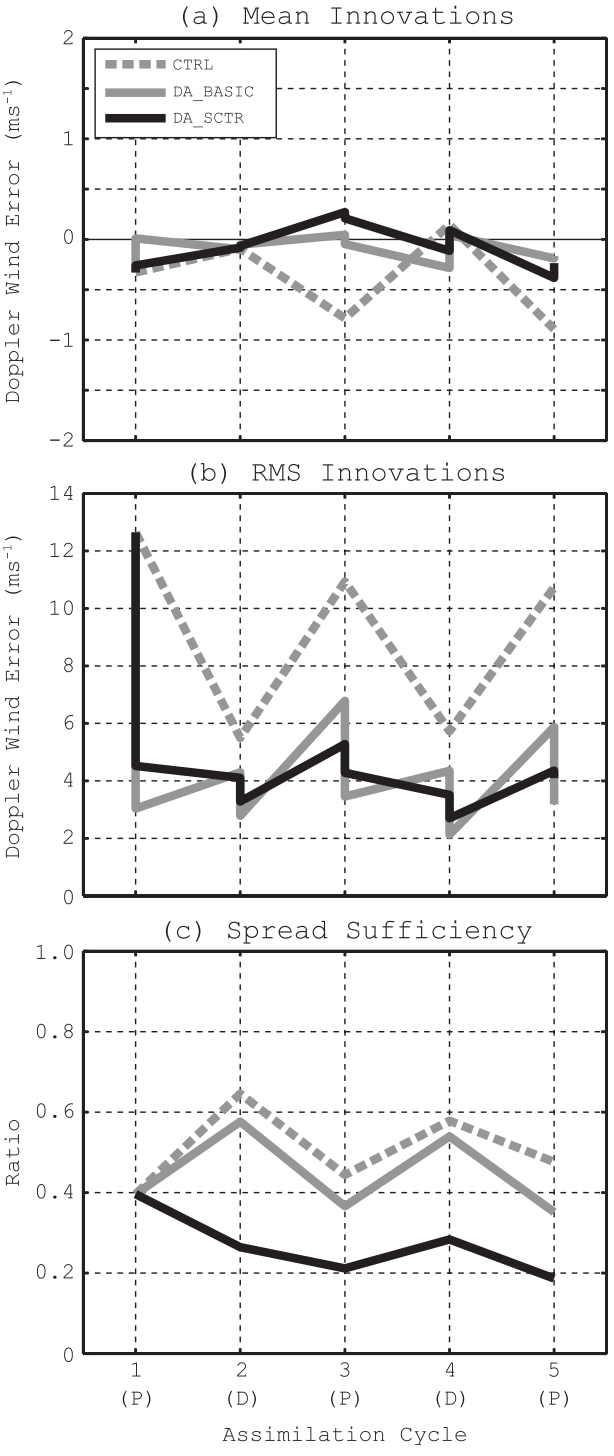

FIG. 3. Observation-space diagnostics for Doppler radial wind observations: (a) mean innovations, (b) RMS innovations, and (c) spread sufficiency. The statistics are computed at the same randomly selected locations that were not assimilated but were within the same physical region as the assimilated observations in DA_BASIC. Letters P and D beneath assimilation cycle numbers indicate whether these verification data are primarily composed of observations from penetration or downwind legs, respectively.

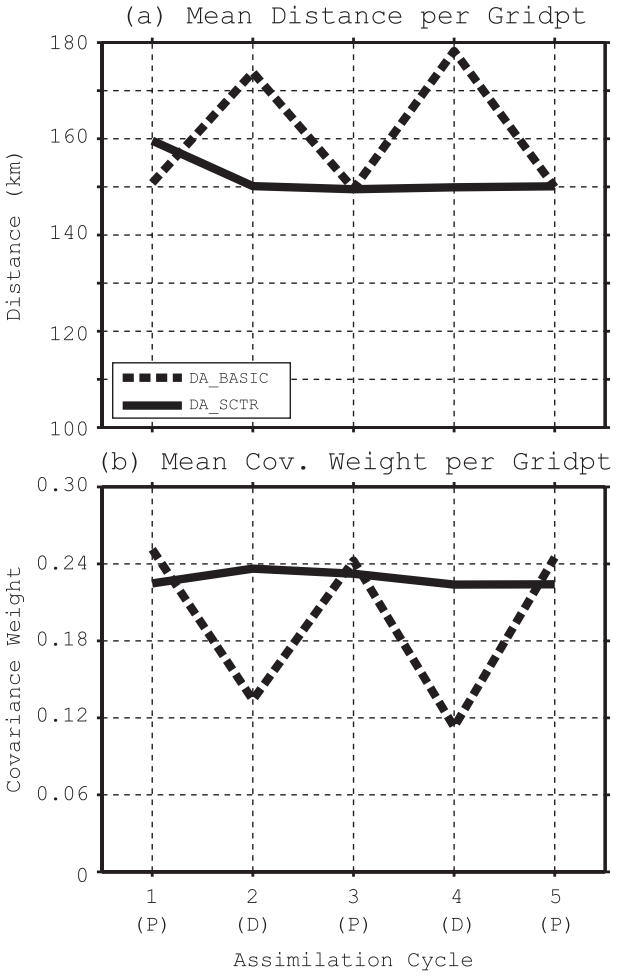

FIG. 4. Comparison between DA_BASIC (dashed lines) and DA_SCTR (solid lines) for (a) mean observation–gridpoint distance per grid point updated, and (b) mean covariance localization weight applied to each grid point updated.

asymmetric distribution of observations within the vortex in DA_BASIC. The greater average covariance weight in DA_SCTR effectively results in a relatively greater reduction in ensemble spread during the EnKF updates in cycles 2 and 4.

2) MODEL-SPACE DIAGNOSTICS

A direct comparison of model variables is performed by computing mean errors with reference to the nature run (Fig. 5). As in A12, statistics are computed in storm-relative cylindrical coordinates (0–300 km radially at 1-km resolution, 0°–360° azimuthally at 1° resolution, and 1–20 model levels vertically through the middle troposphere). Error statistics are computed only for the tail of the distributions of some of the key model variables, such as *absolute* zonal wind speed $|u|$, updraft speed w^+, and absolute perturbations (from azimuthally

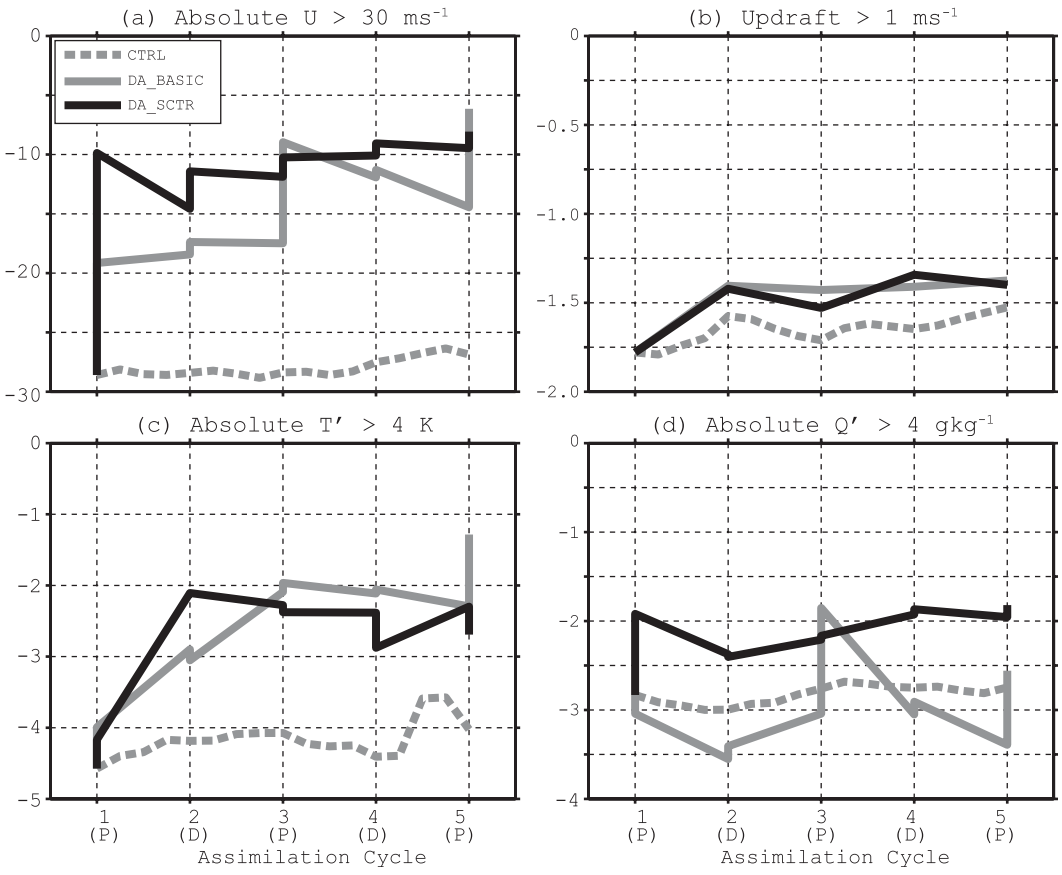

FIG. 5. Mean difference from the nature run for (a) absolute u component of horizontal wind greater than 30 m s^{-1} in the nature run, (b) updraft speed greater than 1 m s^{-1}, (c) absolute perturbation temperature greater than 4 K, and (d) absolute perturbation specific humidity greater than 4 g kg^{-1}. Computations are performed in storm-relative coordinates within 300 km radially of respective storm centers.

averaged values of 300 km from the TC center) of temperature $|T'|$ and specific humidity $|q'|$ by applying threshold values of 30 m s^{-1}, 1 m s^{-1}, 4 K, and 4 g kg^{-1}, respectively. These thresholds are chosen so that 2%–3% of the total population of respective variables is considered, roughly corresponding to outliers of twice the standard deviation or more (see A12 for further details). ''Mean error'' in this context refers to an average of experiment–nature differences for those grid points in the nature run that are thresholded at the mentioned values.

Results suggest generally positive impact from storm-relative data assimilation, especially for $|u|$ and $|q'|$. For $|u|$, a generally lower mean error of ~5 m s^{-1} is observed throughout the assimilation cycles, and the final analysis mean error in DA_SCTR is comparable to DA_BASIC. For $|q'|$, compared to DA_BASIC, an overall reduction in mean error of ~0.5 g kg^{-1} is persistent and is also apparent in the final analysis in DA_SCTR. This is especially promising considering that an improvement in $|T'|$ was already accomplished in DA_BASIC.

In an average sense, the $|u|$ and $|q'|$ fields also demonstrate slower cycle-to-cycle error growth in DA_SCTR compared to DA_BASIC (Figs. 5a and 5d). This supports the hypothesis that a smoother transition from analyses to short-range forecasts is possibly achieved as a result of storm-relative data assimilation.

Further model-based diagnostics are performed for parameters that describe certain storm characteristics (Fig. 6). Here, six parameters are chosen that demonstrate the most impact in DA_BASIC in A12: minimum sea level pressure (MSLP), maximum azimuthally averaged tangential wind speed (VTmax), maximum 10-m wind speed (V10max), maximum updraft speed (Wmax), radius of maximum azimuthally averaged tangential wind speed (radius of maximum wind or RMW), and the depth of the inflow layer at the RMW (VRrmw_hgt).

Distinct improvements, especially in early cycles, are observed in MSLP and VTmax. In addition, these two

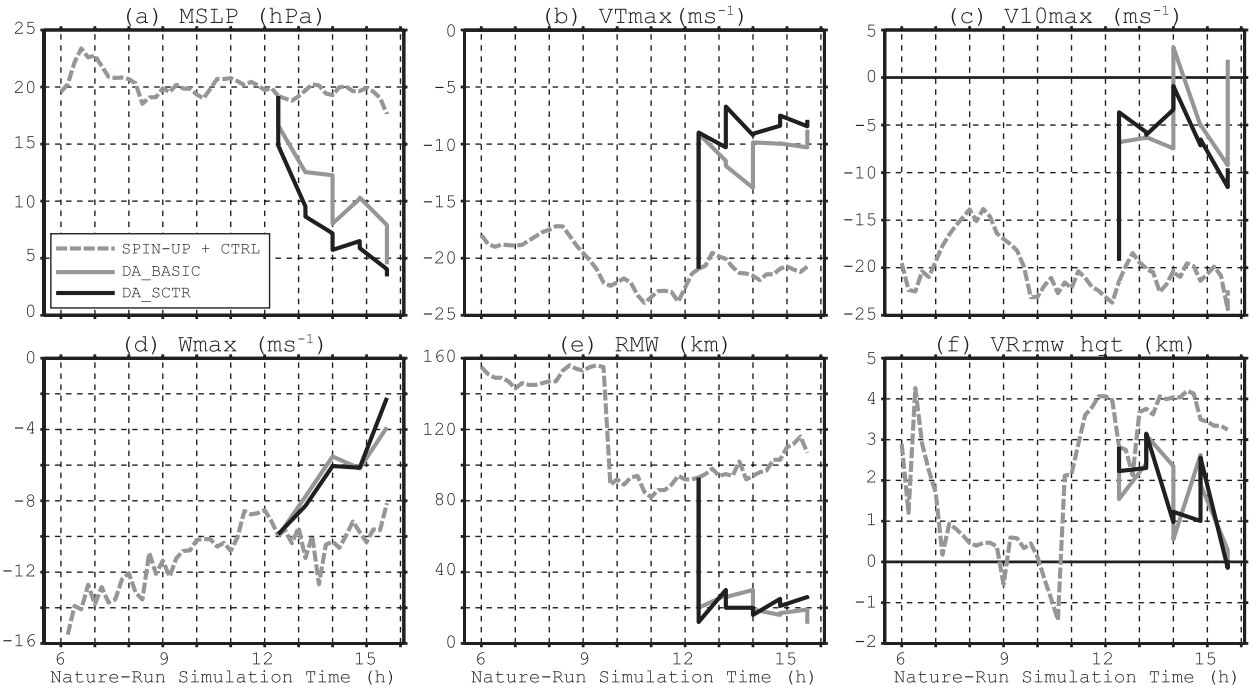

FIG. 6. Deviations from the nature run for (a) MSLP, (b) VTmax, (c) V10max, (d) Wmax, (e) RMW, and (f) VRrmw_hgt. Time along the *x* axis denotes hours since the start of the nature run simulation.

parameters also exhibit slower cycle-to-cycle error growth than DA_BASIC, consistent with what was observed in $|u|$ previously.

As these two variables appear to be well correlated in how they respond to storm-relative data assimilation, one could perhaps conjecture that no distinct changes in errors related to RMW should be seen, as a stronger tangential wind speed (deduced from smaller error) only implies a stronger pressure gradient and the stronger pressure gradient would only result in a deeper central pressure if RMW stayed roughly the same. This is indeed what happens to RMW in the DA_SCTR experiment, compared to DA_BASIC.

Meanwhile, the DA_SCTR experiment appears to have minimal impact on V10max, Wmax, and VRrmw_hgt. The lack of impact on V10max despite the positive impact on MSLP and VTmax is interesting and points to the differences in the representativeness of these quantities in general. We find VTmax, being an azimuthally averaged quantity, and MSLP, being a column-integral quantity, represent the ''broader'' vortex properties better than V10max. They are therefore believed to be more likely to respond to storm-relative data assimilation due to the more homogeneous distribution of observations across the vortex. But at the same time, some spatiotemporal smoothing is likely as observations from the entire 4-h flight are randomly assigned to assimilation cycles. On the other hand, V10max represents smaller-scale features of the vortex both spatially and temporally and, therefore, is likely impacted less by the storm-relative data assimilation due to the resulting spatial–temporal smoothing.

b. *Impact of number of observations, covariance relaxation, and covariance localization*

As observed in the previous section, the decrease in ensemble spread in DA_SCTR compared to DA_BASIC is believed to be related to the smaller average distance to the observations per model grid point. Clearly, a fair comparison between DA_BASIC and DA_SCTR has to involve accounting for such differences in the data assimilation. In this section, such a comparison is performed by varying certain aspects of the data assimilation system in HEDAS. This is done for the number of observations assimilated, inflation of the background covariances through covariance relaxation (Zhang et al. 2004), and the horizontal covariance localization length scale.

The investigation is first carried out in observation space in terms of RMS innovations and spread sufficiency (Fig. 7). All appear to improve the spread sufficiency to varying degrees, the greatest relative impact resulting from covariance relaxation while the smallest from the number of observations assimilated. Meanwhile, the impact on RMS innovations is limited in all cases and almost nonexistent for the number of observations assimilated. Moderate amounts of covariance

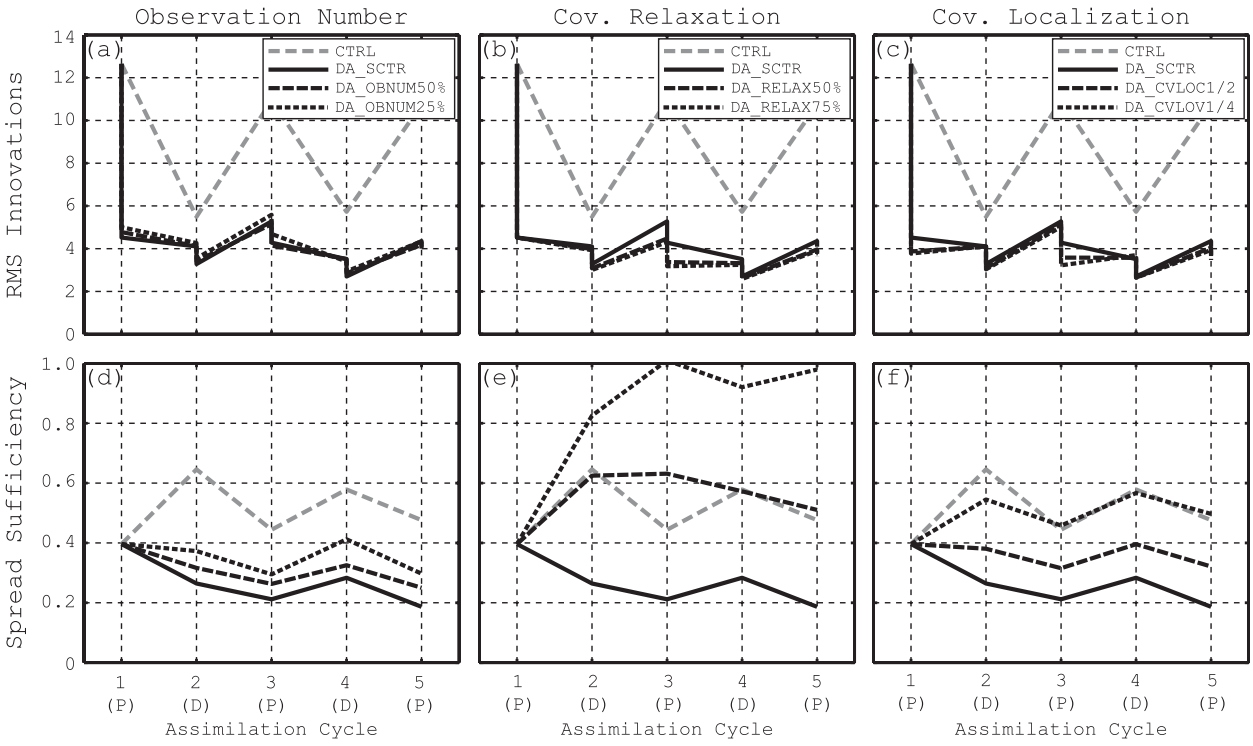

FIG. 7. (a)–(c) Observation-space RMS innovations and (d)–(f) spread sufficiency for the comparison of variations in (left) assimilated observation number, (middle) covariance relaxation, and (right) horizontal covariance localization.

relaxation (DA_RELAX50%) and reduction in covariance localization length scale (DA_CVLOC1/2) appear to lead to improvements during the early cycles.

In model space, the impact is generally more pronounced (Fig. 8). In terms of $|u|$ mean error with 30 m s^{-1} threshold, the mean analysis error is reduced by up to 5 m s^{-1} for both covariance relaxation and covariance localization. However, error reduction is better maintained during short-range forecasts in the covariance localization experiments, with DA_CVLOC1/2 resulting in the largest relative positive impact on the mean error. There are also improvements of 0.5–1 K in the mean error of $|T'|$ in covariance relaxation and covariance localization experiments, where no noticeable improvements in this variable were observed in DA_SCTR. However, these improvements are accompanied by small degradations in $|q'|$ mean error. It appears that the overall impact on the thermodynamic properties of the vortex from storm-relative data assimilation is mostly inconclusive.

The impacts on VTmax, V10max, and RMW are also examined (Fig. 9). The results are similar to previous findings, and the number of observations assimilated has very little overall impact on the size or the intensity of the vortex. Meanwhile, introducing covariance relaxation and reducing covariance localization both appear to positively impact intensity and size. Consistent with the improvements in $|u|$, the results for covariance localization are more persistent and the DA_CVLOC1/2 leads to the largest incremental improvement. Improvements are also more general in the sense that VTmax, V10max, and RMW all appear to be positively impacted. Errors in VTmax, V10max, and RMW are reduced by 3–4 m s^{-1}, 2–3 m s^{-1}, and 20 km, respectively, compared to the DA_SCTR experiment.

c. *Comparison of final mean analyses*

The focus is now turned to the properties of the final mean analysis in comparison to the vortex in the nature run and the DA_BASIC experiment from A12. The final mean analysis of the DA_CVLOC1/2 experiment is used here, as this experiment resulted in the best improvements in both observation and model spaces. Treating spread deficiency through a reduction in the length scale of horizontal covariance localization is also preferred here as it better counteracts the deterioration of the spread sufficiency in DA_SCTR from the smaller average distance to observations per model grid point in storm-relative data assimilation.

Figure 10 compares horizontal cross sections of 10-m wind speed and 1-km total cloud water mass (CWM).

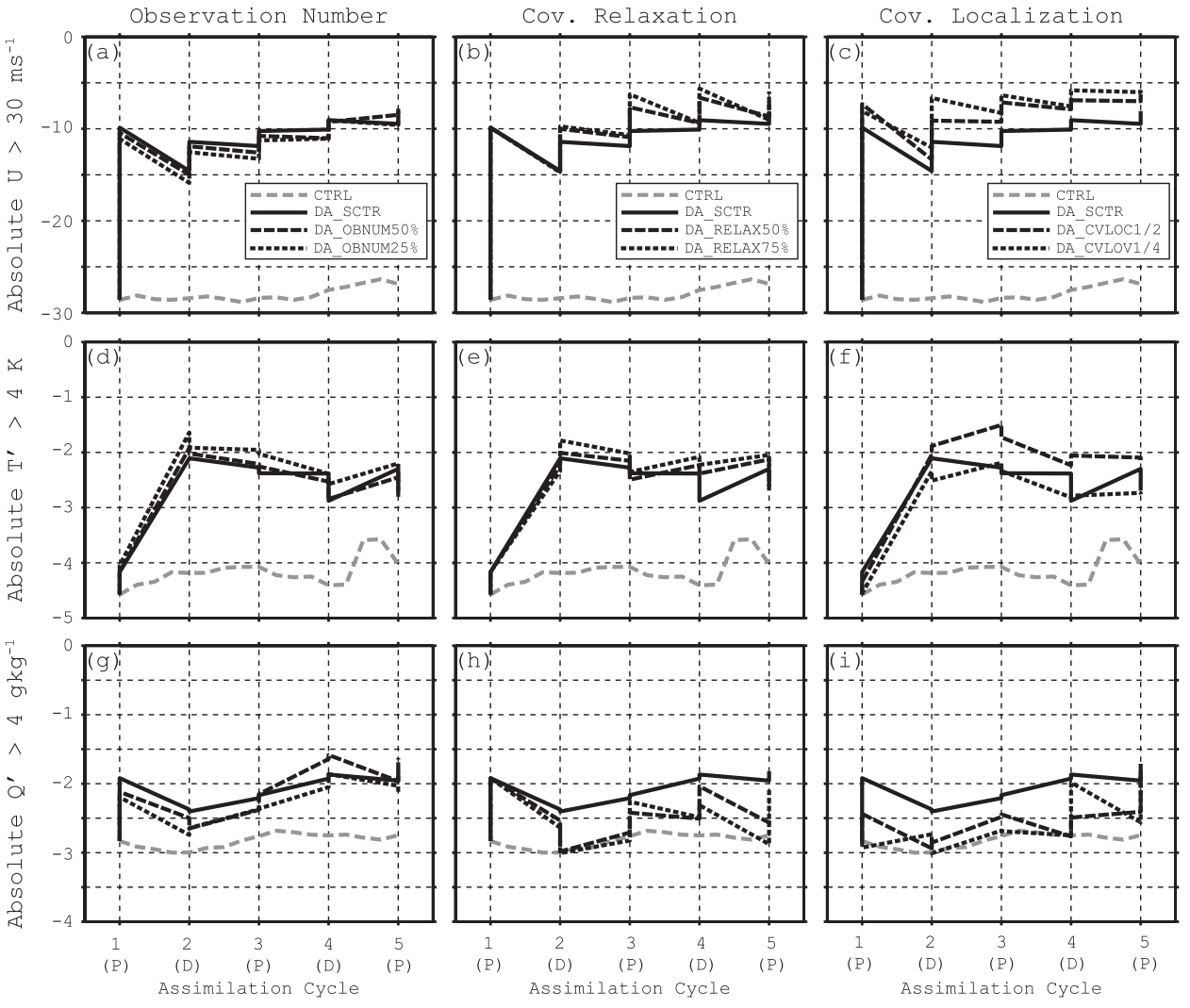

FIG. 8. As in Fig. 7, but for the mean difference from the nature run for the (a)–(c) absolute u component of horizontal wind greater than 30 m s^{-1} in the nature, (d)–(f) absolute perturbation temperature greater than 4 K, and (g)–(i) absolute perturbation specific humidity greater than 4 g kg^{-1}.

The final analysis of 10-m wind speed in DA_CVLOC1/2 appears to be distinctly smoother than in DA_BASIC. The shapes of the eye and the eyewall are also better captured in DA_CVLOC1/2. The CWM analysis in DA_CVLOC1/2 also supports a better representation of an eyewall structure compared to DA_BASIC. In addition, the rain-free regions west and south of the vortex observed in the nature run appear to be better analyzed in DA_CVLOC1/2.

Figure 11 compares vertical cross sections of azimuthally averaged tangential and radial wind speeds, as well as equivalent potential temperature θ_e. The tangential wind speed in DA_CVLOC1/2 reveals a vortex structure that better extends vertically and is slightly less tilted than DA_BASIC in general. Both DA_CVLOC1/2 and DA_BASIC appear to underanalyze the maximum tangential wind speed. Meanwhile, the results in the distribution of the radial wind speed are somewhat mixed. While the final mean analysis in DA_CVLOC1/2 contains a more radially uniform boundary layer inflow layer of magnitude 5–7.5 m s^{-1}, the upper-level outflow is distinctly weaker by ~2.5 m s^{-1}. Similarly mixed results are obtained in the analysis of the thermodynamic structure of the vortex. The low-to-midlevel warm core is weaker by 5–10 K in DA_CVLOC1/2 but with a better vertical extent (the 350-K contour reaches 2 km higher in DA_CVLOC1/2 than in DA_BASIC, and is more consistent with the nature run). There is also a better-represented upper-level warming in

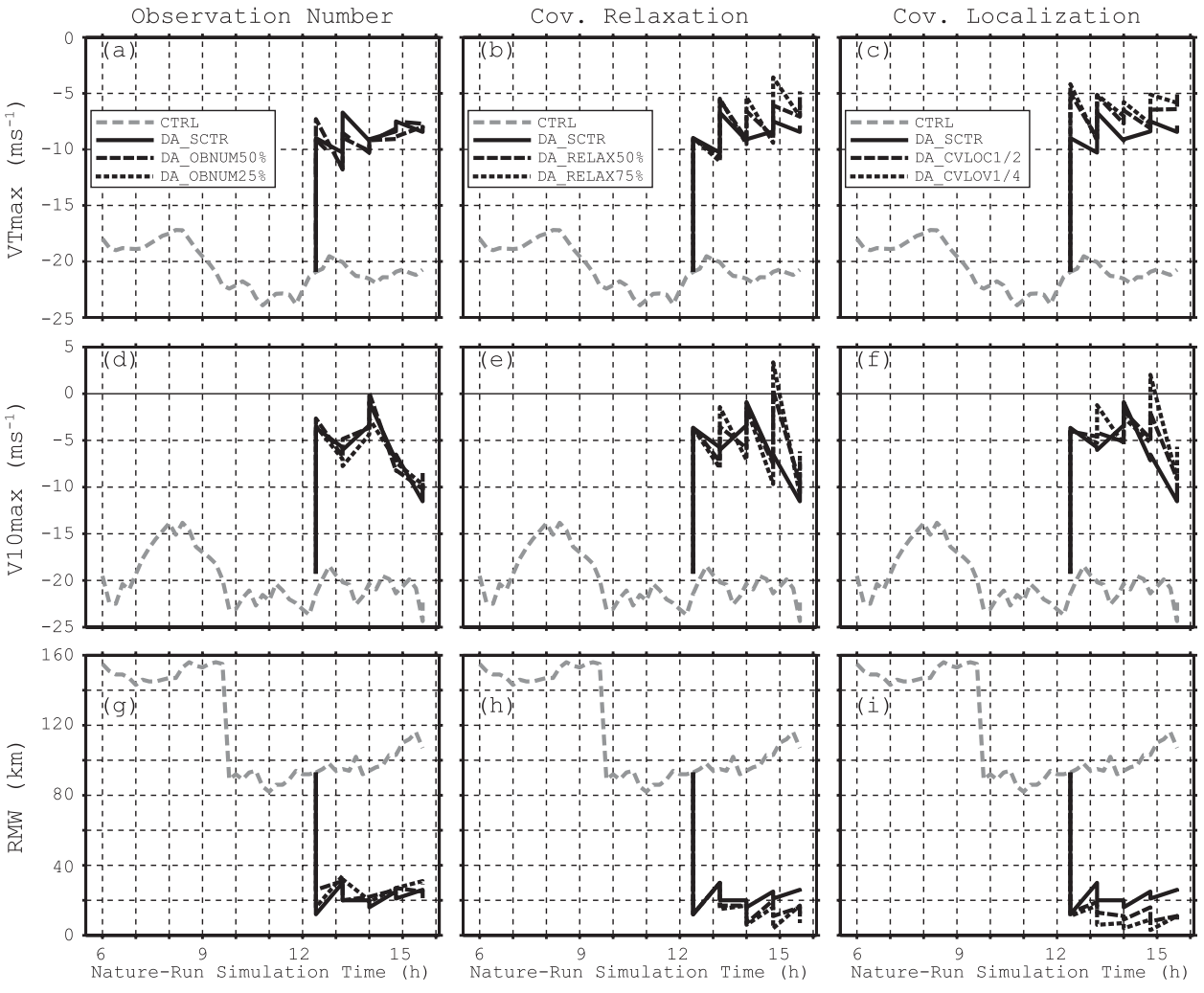

FIG. 9. As in Fig. 7, but for the deviations from the nature run for (a)–(c) VTmax, (d)–(f) V10max, and (g)–(i) RMW.

DA_CVLOC1/2, consistent with a deeper warm-core vortex structure.

Overall, the vortex structure analyzed in DA_CVLOC1/2 is believed to exhibit realistic kinematic and thermodynamic fields that are consistent with their counterparts in the nature run. A deeper and less tilted tangential wind speed structure is supported with a boundary layer inflow layer that is more uniform radially. Although not as strong as in the nature run, the warm-core structure has better vertical extent in DA_CVLOC1/2 and exhibits signs of upper-level warming in the core. Such structural consistency with the nature run could be a precursor for the slower cycle-to-cycle error growth previously observed in both observation space and in mode space. To investigate this possibility further, the next section compares how certain fields change on average in the short-range forecasts during cycling.

d. On the analysis-to-forecast transition during cycling

Figure 12 compares the vertical cross sections of the change in azimuthally averaged tangential and radial wind speeds, as well as θ_e, during short-range forecasts by averaging the forecast-minus-analysis differences from cycles 2 through 5. To perform structurally consistent comparisons, radial distances from the TC center are normalized by the respective RMWs at each time before averaging. These average differences are used as a proxy for how the model transitions from analyses to forecasts during the cycling in HEDAS. For reference, the corresponding average 48-min forecast differences in the nature run are also shown.

The average forecast differences in the nature run in all fields shown are quite small and point to a mostly steady-state nature run vortex structure during cycling.

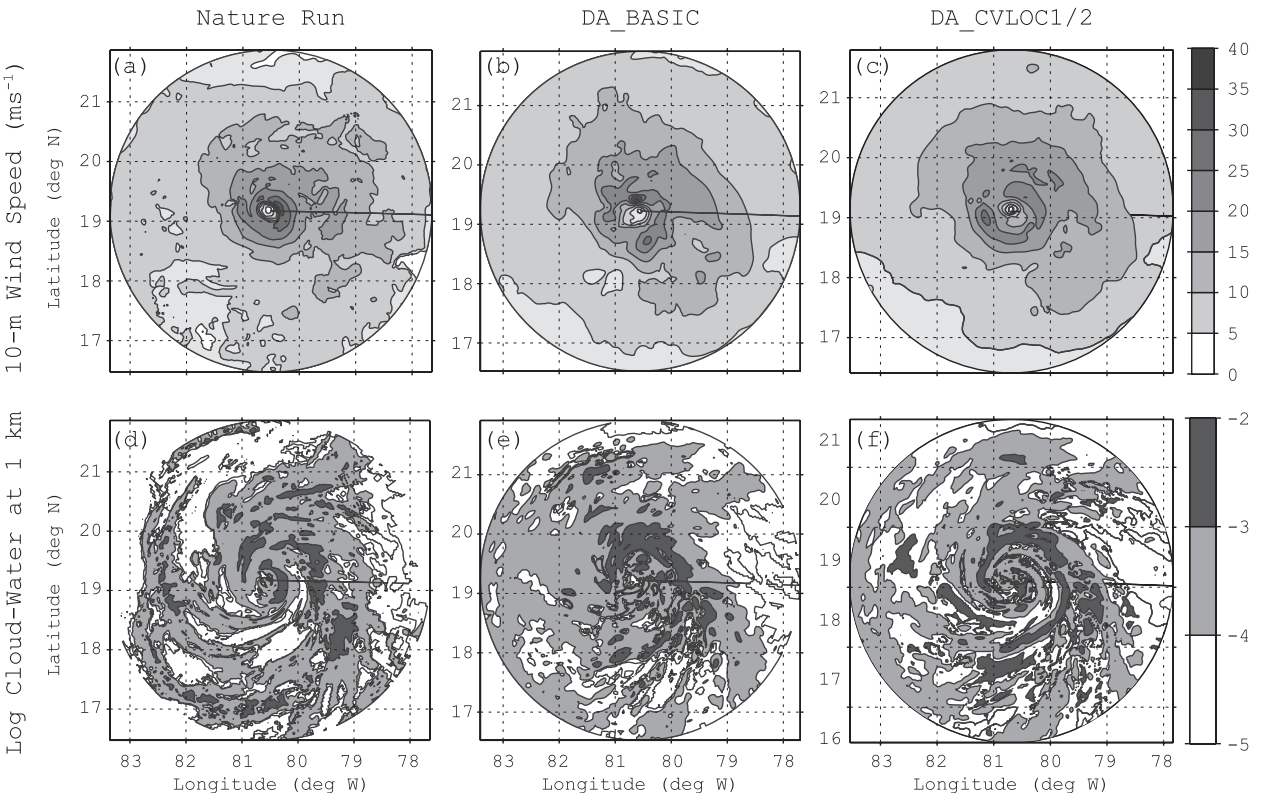

FIG. 10. Storm-relative horizontal cross sections of (a)–(c) 10-m wind speed (m s^{-1}) and (d)–(f) logarithm of 1-km total cloud water mass in the (left) nature run, (middle) final mean analysis in the DA_BASIC experiment, and (right) final mean analysis in the DA_CVLOC1/2 experiment.

The differences are also mostly confined to the TC core, indicating that no significant vortex deformation (e.g., tilting) occurs in the nature run. Therefore, the emergence of any large forecast–analysis differences in the data assimilation experiments should indicate adjustments beyond the nature run tendencies, possibly as a result of improper transitioning from analyses to forecasts during cycling.

In tangential wind speed, both DA_BASIC and DA_CVLOC1/2 exhibit average weakening in the boundary layer during short-range forecasts, although the weakening in DA_CVLOC1/2 is smaller by ~1 m s^{-1}. This smaller average weakening is also accompanied by strengthening near the RMW higher up. Although DA_BASIC also exhibits strengthening higher up, it occurs radially farther out at ~2 RMW. The combination of a larger weakening near the boundary layer and strengthening that is radially displaced is believed to lead to a more distorted primary circulation in DA_BASIC during the short-range forecasts.

Weakening is also observed in radial inflow in the boundary layer both for DA_BASIC and DA_CVLOC1/2. But again, the weakening is more pronounced in DA_BASIC. The upper-level outflow in DA_CVLOC1/2 also weakens (positive values point to weakening as radial outflow is represented with negative values; cf. to Figs. 11d–f) but by a greater extent than DA_BASIC. In general, the response of the evolution of the secondary circulation in short-range forecasts to storm-relative data assimilation appears to be less conclusive than the response in the primary circulation.

Finally, in terms of θ_e, a more distinct low-to-midlevel warming occurs in DA_CVLOC1/2. Considering that the strength of the warm core in the same region in the final analysis is underanalyzed, this warming likely brings the vortex to better consistency between kinematic and thermal structures. Moreover, the DA_BASIC exhibits some cooling in the boundary layer radially away from the core, which is not existent in DA_CVLOC1/2.

Overall, the primary circulation in the DA_CVLOC1/2 experiment remains vertically better aligned at around RMW during the short-range forecasts than DA_BASIC and experiences smaller weakening. The forecast evolution of the thermodynamic structure in DA_CVLOC1/2 appears to be better confined to the TC core (to within ~1 RMW), consistent with the evolution of the primary

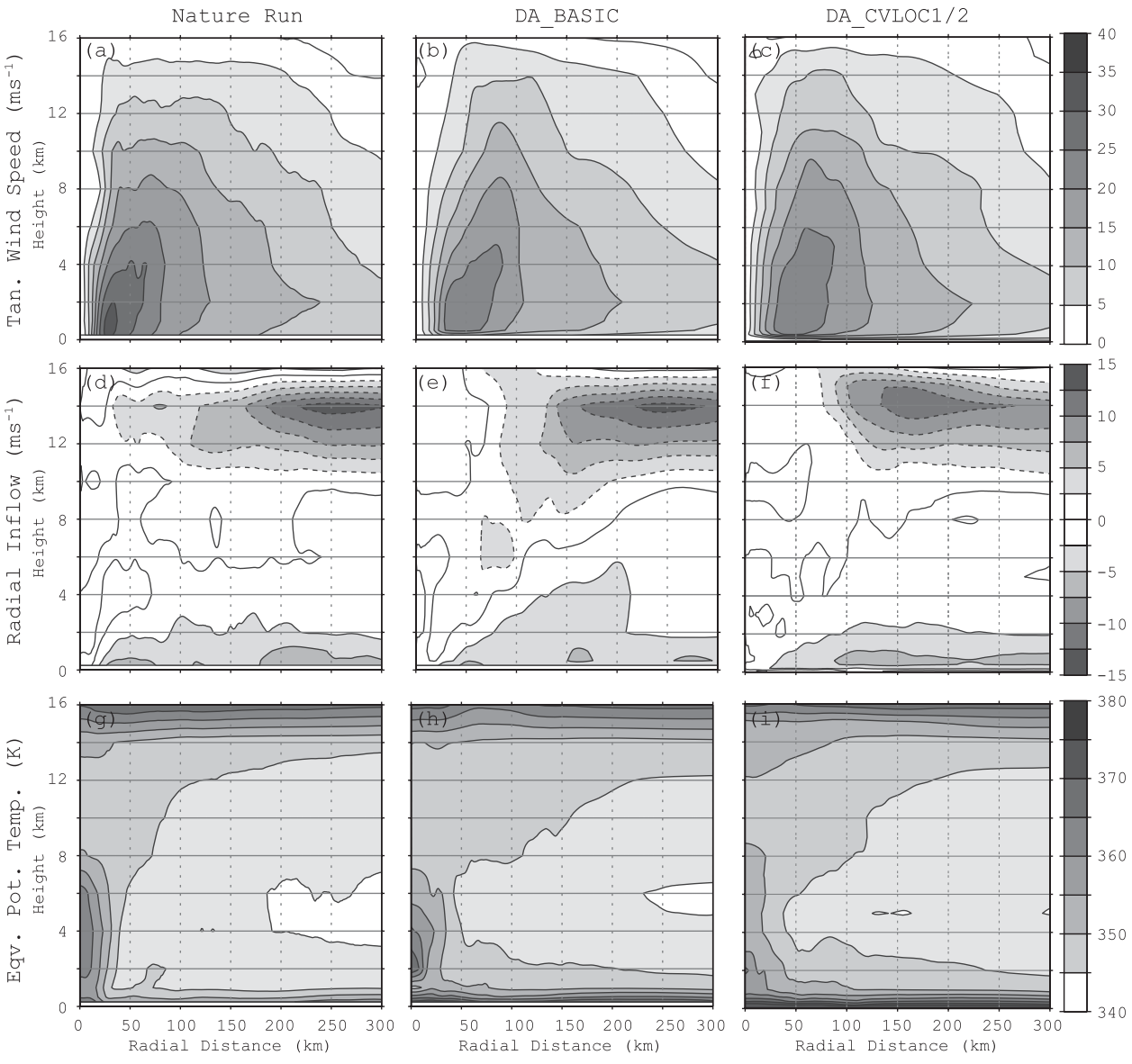

FIG. 11. Vertical cross sections of (a)–(c) azimuthally averaged tangential wind speed (m s^{-1}), (d)–(f) radial inflow (m s^{-1}), and (g)–(i) equivalent potential temperature (K). (left) The nature run, (middle) the final mean analysis in the DA_BASIC experiment, and (right) the final mean analysis in the DA_CVLOC1/2 experiment.

circulation structure. These findings suggest that, with storm-relative data assimilation, the vortex evolution during the short-range forecasts remains more consistent with the steady-state nature of the nature run in DA_CVLOC1/2 and may be a manifestation of a smoother transitioning from analyses to forecasts.

5. Summary and discussion

In this study, storm-relative TC data assimilation is introduced for the EnKF using NOAA/AOML/HRD's HEDAS. It entails translating observations to a common storm center by maintaining their storm-relative position as of the time of their actual sampling. This requires the assumption of the simultaneity of all observations in a TC. The observations are then randomly redistributed to assimilation cycles to achieve a spatially more homogeneous distribution. The current proof-of-concept study is carried out in an OSSE with the same nature run simulation and simulated airborne Doppler radar wind superobservations as in A12. The results here are compared to A12's earth-relative version of HEDAS.

The direct implementation of storm-relative data assimilation to the HEDAS configuration as in A12 (their

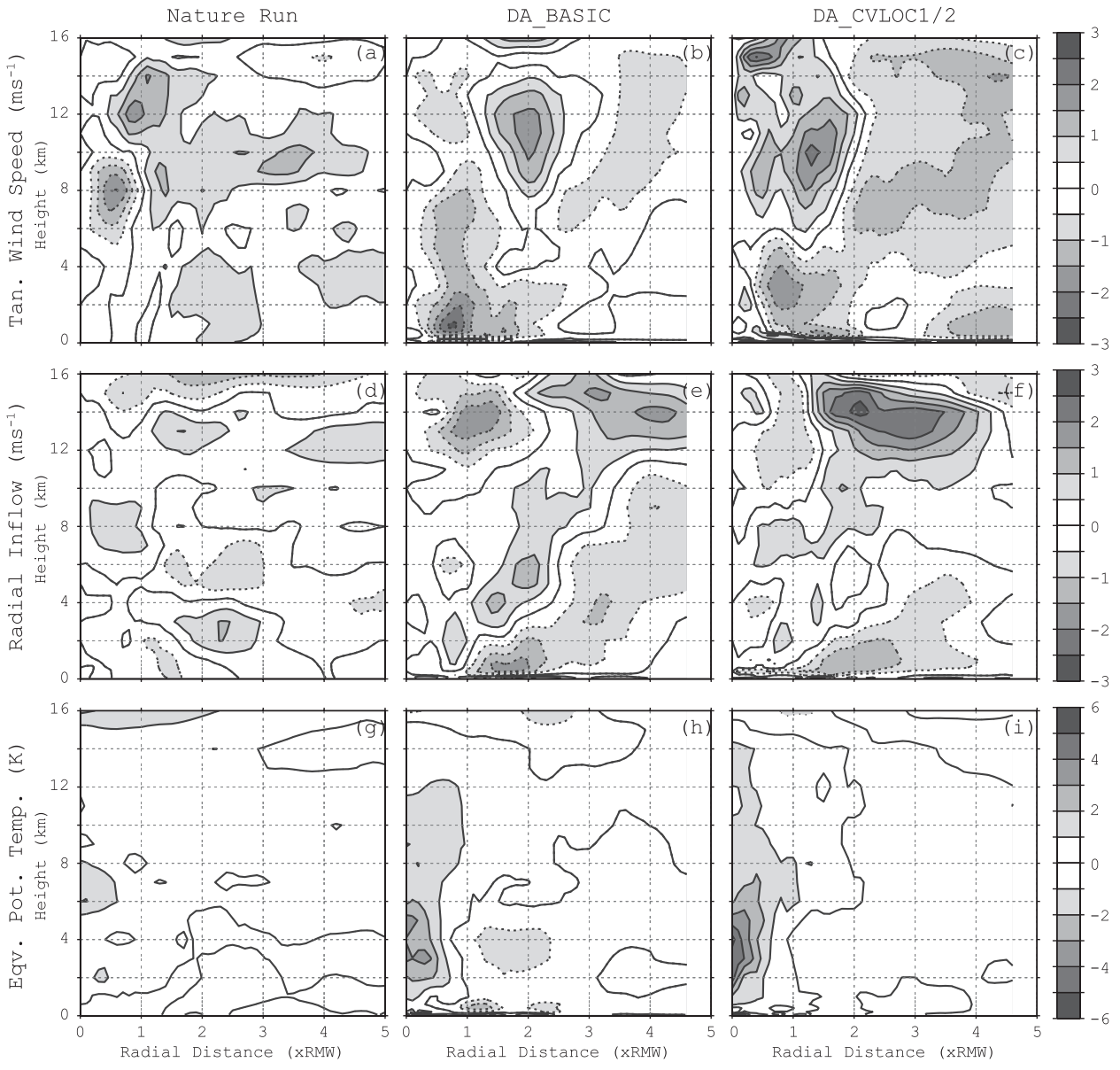

FIG. 12. Vertical cross sections of four-cycle average differences between 48-min forecasts and analyses of (a)–(c) azimuthally averaged tangential wind speed (m s^{-1}), (d)–(f) radial inflow (m s^{-1}), and (g)–(i) equivalent potential temperature (K). (left) The corresponding average 48-min forecast differences in the nature run, (middle) the DA_BASIC experiment, and (right) the DA_CVLOC1/2 experiment. Horizontal axes denote radial distances from storm center normalized by the RMW.

DA_BASIC experiment) reveals improvements in the kinematic representation of the TC vortex analyses, while the overall impact on the thermodynamic properties is mostly inconclusive. The greatest positive impact is seen in the slower cycle-to-cycle error growth when storm-relative data assimilation is applied. This method also leads to a reduction in ensemble spread during cycling. This is believed to be due to the more homogeneous distribution of observations in each assimilation cycle: the average distance to observations per grid point is reduced, resulting in greater average weight applied to covariances per grid point and therefore, by design, smaller analysis variance.

The homogeneous spatial distribution of observations also allows a more vigorous testing of various methods to encounter spread deficiency as the earth-relative framework of A12 forced the choice of a large enough horizontal covariance localization length scale to counteract the asymmetrical distribution of observations in assimilation cycles. When various experiments are

performed within a storm-relative framework, modest amounts of covariance relaxation (50%) and reduction of the horizontal covariance localization length scale (by ½ to ~120 km) are observed to result in the greatest incremental improvements both in observation space and in model space, leading to a better representation of both the vortex primary circulation strength and size.

The final mean analysis of the experiment with ½ the original covariance localization length scale also exhibits an improved vortex structure. Horizontally, the 10-m wind speed distribution is smoother and contains a better-defined maximum-wind region with asymmetries that match those in the nature run. A more realistic eyewall structure is also observed in the total cloud condensate. The azimuthally averaged tangential wind speed reveals a vortex structure that better extends vertically and is slightly less tilted in general. The warm-core structure, too, while somewhat underanalyzed in magnitude, better conforms vertically with the kinematic vortex.

It is also not very surprising that a smaller covariance localization length scale leads to better improvements in observation and model space than applying covariance relaxation or thinning the number of observations assimilated, as the worsened spread deficiency is, at least partially, due to the reduced average distance to observations per model grid point. The emerging ''optimal'' covariance length scale is ~120 km, implying that every Doppler radar wind observation near the TC core is expected to influence the entire inner core during the filter update (for RMW up to 30 km in typical Atlantic hurricanes).

One of the noteworthy results from storm-relative data assimilation appears to be in the smoother transitions of analyses to subsequent short-range forecasts during cycling. This is an important desired property of EnKF-based data assimilation systems as the short-range cycling of observations is critical in achieving balance in the analyses with respect to model dynamics. The apparent smoother analysis-to-forecast transitioning is seen as a promising characteristic in this regard. However, a more vigorous dynamical analysis is needed to diagnose conclusively how balanced the analyses are in HEDAS. This is clearly beyond the scope of the current study and will be the subject of future work.

It should be also underlined that the current storm-relative application, which considers all aircraft observations from a 4–5-h flight as simultaneous, naturally emphasizes vortex features that vary on characteristic time scales that are controlled by the rotational inertial period. Defining ''vortex scale'' as such, variables with overturning time scales that are much shorter than the rotational inertial period, such as mass fields moisture and precipitation that are distributed by convection or turbulence, are expected to be resolved not as optimally within the current data assimilation framework. It is also conceivable that this technique may have limitations during rapid intensification events. Further research is needed to address such limitations. One potential improvement may come from assimilating reflectivity in addition to Doppler radial wind to better constrain the precipitation-related fields in the analysis.

Finally, as storm-relative data assimilation shows promise in this proof-of-concept study, the next step will be to implement it in real-data cases for a more vigorous comparison of its impacts. There are also consequences for how observations are processed in real time, as the storm-relative method described here requires waiting for all observations to be transmitted before they can be processed and assimilated into HEDAS. While this would amount to a delay in the onset of HEDAS in real time compared to the default earth-relative framework, quicker EnKF processes through shorter covariance localization length scales can potentially offset this delay, as the EnKF is the most computationally demanding component of the HEDAS infrastructure. A quantitative analysis of these various aspects of computational performance in HEDAS is deferred to a future study with real data.

Acknowledgments. The author acknowledges funding from the NOAA Hurricane Forecast Improvement Project that supported this work. This research was carried out (in part) under the auspices of CIMAS, a joint institute of the University of Miami and NOAA (Cooperative Agreement NA67RJ0149). Insightful comments from Drs. Sylvie Lorsolo, Sim Aberson, and Tomislava Vukicevic from NOAA/AOML/HRD were very helpful in improving preliminary versions of the manuscript. Comments from three anonymous reviewers that helped to refine the manuscript are also acknowledged.

REFERENCES

Aberson, S. D., 2010: 10 years of hurricane synoptic surveillance (1997–2006). *Mon. Wea. Rev.,* **138,** 1536–1549.

——, M. L. Black, R. A. Black, R. W. Burpee, J. J. Cione, C. W. Landsea, and F. D. Marks Jr., 2006: Thirty years of tropical cyclone research with the NOAA P-3 aircraft. *Bull. Amer. Meteor. Soc.,* **87,** 1039–1055.

Aksoy, A., D. Dowell, and C. Snyder, 2009: A multicase comparative assessment of the ensemble Kalman filter for assimilation of radar observations. Part I: Storm-scale analyses. *Mon. Wea. Rev.,* **137,** 1805–1824.

——, S. Lorsolo, T. Vukicevic, K. Sellwood, S. Aberson, and F. Zhang, 2012: The HWRF Hurricane Ensemble Data Assimilation System (HEDAS) for high-resolution data: The

impact of airborne Doppler radar observations in an OSSE. *Mon. Wea. Rev.,* **140,** 1843–1862.

Berg, R. J., and L. A. Avila, 2011: Atlantic hurricane season of 2009. *Mon. Wea. Rev.,* **139,** 1049–1069.

Cline, I. M., 1926: *Tropical Cyclones*. MacMillan, 301 pp.

Daley, R., 1991: *Atmospheric Data Analysis*. Cambridge University Press, 457 pp.

Demuth, J., M. DeMaria, and J. A. Knaff, 2006: Improvement of Advanced Microwave Sounder Unit tropical cyclone intensity and size estimation algorithms. *J. Appl. Meteor.,* **45,** 1573–1581.

Dowell, D. C., F. Zhang, L. J. Wicker, C. Snyder, and N. A. Crook, 2004: Wind and temperature retrievals in the 17 May 1981 Arcadia, Oklahoma, supercell: Ensemble Kalman filter experiments. *Mon. Wea. Rev.,* **132,** 1982–2005.

Gaspari, G., and S. E. Cohn, 1999: Construction of correlation functions in two and three dimensions. *Quart. J. Roy. Meteor. Soc.,* **125,** 723–757.

Gopalakrishnan, S. G., and Coauthors, 2002: An operational multiscale hurricane forecasting system. *Mon. Wea. Rev.,* **130,** 1830–1847.

——, N. Surgi, R. Tuleya, and Z. Janjic, 2006: NCEP's two-way-interactive-moving-nest NMM-WRF modeling system for hurricane forecasting. Preprints, *27th Conf. on Hurricanes and Tropical Meteorology,* Monterey, CA, Amer. Meteor. Soc., 7A.3. [Available online at http://ams.confex.com/ams/pdfpapers/107899.pdf.]

——, F. Marks Jr., X. Zhang, J.-W. Bao, K.-S. Yeh, and R. Atlas, 2011: The experimental HWRF system: A study on the influence of horizontal resolution on the structure and intensity changes in tropical cyclones using an idealized framework. *Mon. Wea. Rev.,* **139,** 1762–1784.

Hamill, T. M., and J. S. Whitaker, 2005: Accounting for the error due to unresolved scales in ensemble data assimilation: A comparison of different approaches. *Mon. Wea. Rev.,* **133,** 3132–3147.

——, ——, M. Fiorino, and S. G. Benjamin, 2011: Global ensemble predictions of 2009's tropical cyclones initialized with an ensemble Kalman filter. *Mon. Wea. Rev.,* **139,** 668–688.

Jones, S. C., 1995: The evolution of vortices in vertical shear. I: Initially barotropic vortices. *Quart. J. Roy. Meteor. Soc.,* **121,** 821–851.

Kalnay, E., 2006: *Atmospheric Modeling, Data Assimilation and Predictability*. Cambridge University Press, 341 pp.

Kaplan, J., M. DeMaria, and J. A. Knaff, 2010: A revised tropical cyclone rapid intensification index for the Atlantic and eastern North Pacific basins. *Wea. Forecasting,* **25,** 220–241.

Mallen, K. J., M. T. Montgomery, and B. Wang, 2005: Reexamining the near-core radial structure of the tropical cyclone primary circulation: Implications for vortex resiliency. *J. Atmos. Sci.,* **62,** 408–425.

Marks, F. D., Jr., P. G. Black, M. T. Montgomery, and R. W. Burpee, 2008: Structure of the eye and eyewall of Hurricane Hugo (1989). *Mon. Wea. Rev.,* **136,** 1237–1259.

Nguyen, S. V., R. K. Smith, and M. T. Montgomery, 2008: Tropical-cyclone intensification and predictability in three dimensions. *Quart. J. Roy. Meteor. Soc.,* **134,** 563–582.

Reasor, P. D., M. T. Montgomery, and L. D. Grasso, 2004: A new look at the problem of tropical cyclones in vertical shear flow: Vortex resiliency. *J. Atmos. Sci.,* **61,** 3–22.

Rogers, R., 2010: Convective-scale structure and evolution during a high-resolution simulation of tropical cyclone rapid intensification. *J. Atmos. Sci.,* **67,** 44–70.

Stern, D. P., and D. S. Nolan, 2009: Reexamining the vertical structure of tangential winds in tropical cyclones: Observations and theory. *J. Atmos. Sci.,* **66,** 3579–3600.

Weng, Y., and F. Zhang, 2012: Assimilating airborne Doppler radar observations with an ensemble Kalman filter for convection-permitting hurricane initialization and prediction: Katrina (2005). *Mon. Wea. Rev.,* **140,** 841–859.

Whitaker, J., and T. M. Hamill, 2002: Ensemble data assimilation without perturbed observations. *Mon. Wea. Rev.,* **130,** 1913–1924.

Xiao, Q., X. Zhang, C. Davis, J. Tuttle G. Holland, and P. J. Fitzpatrick, 2009: Experiments of hurricane initialization with airborne Doppler radar data for the Advanced Research Hurricane WRF (AHW) model. *Mon. Wea. Rev.,* **137,** 2758–2777.

Zhang, F., C. Snyder, and J. Sun, 2004: Impacts of initial estimate and observation availability on convective-scale data assimilation with an ensemble Kalman filter. *Mon. Wea. Rev.,* **132,** 1238–1253.

——, Y. Weng, J. A. Sippel, Z. Meng, and C. Bishop, 2009: Cloud-resolving hurricane initialization and prediction through assimilation of Doppler radar observations with an ensemble Kalman filter. *Mon. Wea. Rev.,* **137,** 2105–2125.

——, ——, J. F. Gamache, and F. D. Marks, 2011: Performance of convection-permitting hurricane initialization and prediction during 2008–2010 with ensemble data assimilation of inner-core airborne Doppler radar observations. *Geophys. Res. Lett.,* **38,** L15810, doi:10.1029/2011GL048469.